3D Tensor Factorization Approach to Single-frame Model-free Blind Image Deconvolution

Ivica Kopriva

Division of Laser and Atomic Research and Development

Ruđer Bošković Institute, Bijenička cesta 54, HR-10000, Zagreb, Croatia

Abstract

By applying bank of 2D Gabor filters to blurred image single frame blind image deconvolution (SF BID) is formulated as 3D tensor factorization (TF) problem with the key contribution that neither origin nor size of the spatially invariant blurring kernel is required to be known or estimated. Mixing matrix, original image and its spatial derivatives are identified from the factors in Tucker3 model of the multi-channel version of the blurred image. Previous approaches to 2D Gabor filter bank-based SF BID relied on 2D representation of the multi-channel version of the blurred image and matrix factorization methods such as nonnegative matrix factorization (NMF) and independent component analysis (ICA). Unlike matrix factorization-based methods 3D TF preserves local structure in the image. Moreover, 3D TF based on PARAFAC model is unique up to permutation and scale under very mild conditions. To achieve this, NMF and ICA respectively require enforcement of sparseness and statistical independence constraints on the original image and its spatial derivatives. These constraints are generally not satisfied. The 3D TF-based SF BID method is demonstrated on experimental defocused RGB image.

OCIS codes: 100.1830; 100.3010; 100.3190; 100.6640; 100.6890.

The purpose of blind image deconvolution (BID) is to reconstruct the original image from an observation degraded by spatially invariant blurring process and noise. Neglecting the noise term the process is modeled as a convolution of a point spread function (PSF) $\mathbf{H}(s,t)$ with an original source image $\mathbf{F}(i_1,i_2)$ as:

$$\mathbf{G}(i_1,i_2) = \sum_{s=-M}^{M} \sum_{t=-M}^{M} \mathbf{H}(s,t)\mathbf{F}(i_1 - s, i_2 - t) \tag{1}$$

where M denotes the PSF support size and $\mathbf{G},\mathbf{F} \in \mathbb{R}_{0+}^{I_1 \times I_2}$. If PSF is known a number of algorithms are available to reconstruct original image $\mathbf{F}$ [1]. When PSF is not available BID algorithms are important [2,3]. BID methods can be divided into those that estimate the blurring kernel $\mathbf{H}$ first and then restore original image by some of the non-blind methods [1], and those that estimate the original image $\mathbf{F}$ and blurring kernel simultaneously. In order to estimate the blurring kernel a support size has either to be given or estimated. Also, quite often *a priori* knowledge about the nature of the blurring process is assumed to be available in order to use appropriate parametric model of the blurring process [2]. That is not always fulfilled in practice. Methods that estimate blurring kernel and original image simultaneously use either statistical or deterministic priors of the original image, the blurring kernel and the noise [2], which leads to a computationally expensive maximum likelihood (ML) estimation. Also, exact distributions of the original image required by ML algorithm are usually unknown. Therefore, an approach was proposed in [4] based on quasi ML with an approximate of the probability density function. It however assumed that original image has sparse distribution. To fulfill this assumption it was proposed in [4] to apply sparsifying transform to blurred image. This requires training data. Multivariate data

analysis methods such as nonnegative matrix factorization (NMF) [5] and independent component analysis (ICA) [6-8] can be used to solve BID problem as a blind source separation (BSS) problem where unknown blurring process is absorbed into a mixing matrix. To realize multi-channel version of the blurred image an approach based on a bank of 2-D Gabor filters was proposed in [9]. It has been the basis of the single frame (SF) BID algorithms in [5,7]. The key insight in [9] was that original image $\mathbf{F}(i_1\text{-}s,i_2\text{-}t)$ can be approximated by Taylor series expansion around $\mathbf{F}(i_1,i_2)$ giving $\mathbf{F}(i_1-s,i_2-t)=\mathbf{F}(i_1,i_2)-s\mathbf{F}_{i_1}(i_1,i_2)-t\mathbf{F}_{i_2}(i_1,i_2)-\ldots$, which enables to re-write (1) as:

$$\mathbf{G}(i_1,i_2)=a_1\mathbf{F}(i_1,i_2)+a_2\mathbf{F}_{i_1}(i_1,i_2)+a_3\mathbf{F}_{i_2}(i_1,i_2)+\ldots \quad (2)$$

where $a_1=\sum_{s=-M}^{M}\sum_{t=-M}^{M}\mathbf{H}(s,t)$, $a_2=-\sum_{s=-M}^{M}\sum_{t=-M}^{M}s\mathbf{H}(s,t)$, $a_3=-\sum_{s=-M}^{M}\sum_{t=-M}^{M}t\mathbf{H}(s,t)$ and $\mathbf{F}_{i_1}$ and $\mathbf{F}_{i_2}$ are spatial derivatives in i_1 and i_2 directions respectively. When Gabor filters are applied on blurred image a new set of observed images is obtained as:

$$\mathbf{G}_{i_3}(i_1,i_2)=a_{i_3,1}\mathbf{F}(i_1,i_2)+a_{i_3,2}\mathbf{F}_{i_1}(i_1,i_2)+a_{i_3,3}\mathbf{F}_{i_2}(i_1,i_2)+\ldots \quad i_3=2,\ldots,I_3 \quad (3)$$

where $a_{i_3,1}=\sum_{s=-M}^{M}\sum_{t=-M}^{M}\mathbf{H}_{i_3}^{'}(s,t)$, $a_{i_3,2}=-\sum_{s=-M}^{M}\sum_{t=-M}^{M}s\mathbf{H}_{i_3}^{'}(s,t)$, $a_{i_3,3}=-\sum_{s=-M}^{M}\sum_{t=-M}^{M}t\mathbf{H}_{i_3}^{'}(s,t)$,

where $\mathbf{H}_{i_3}^{'}(s,t)$ represents convolution of the appropriate i_3-th Gabor filter with $\mathbf{H}(s,t)$. In the to be reported experiment I have used bank of 2D Gabor filters with two spatial frequencies and four orientations, whereas real and imaginary parts of the 2D Gabor filters were used as separate filters. Thus, in overall multi-channel version of the blurred image consisted of I_3=17 images. We refer to [5,7] for more detailed description of the 2D Gabor filter bank. In my previous contributions [5,7] multi-channel version of the blurred image $\mathbf{G}$ was represented in 2D as $\mathbf{G}_{(3)}\in\mathbb{R}^{I_3\times I_1 I_2}$ i.e. $\mathbf{G}_{(3)}$ was a set of I_3 images of the size $I_1\times I_2$ pixels, where first image corresponded with the vectorized blurred image $\mathbf{G}$ and the rest of I_3 images corresponded with

vectorized images obtained after filtering blurred image with 2D Gabor filters. In this letter I represent multi-channel version of the blurred image as a three-way array or a 3D tensor $\underline{\mathbf{G}} \in \mathbb{R}^{I_1 \times I_2 \times I_3}$ with elements $g_{i_1 i_2 i_3}$ where i_1=1,..., I_1, i_2=1,..., I_2, i_3=1, ..., I_3. Each index is called way or mode and number of levels on one mode is called dimension of that mode. Two ways of $\underline{\mathbf{G}}$ are for rows and columns and one way is for image index. This is standard notation adopted for use in multi-way analysis [10]. 2D representation of the multi-channel blurred image has two disadvantages: (*i*) 3D tensor $\underline{\mathbf{G}}$ has to be mapped through 3-mode flattening, also called unfolding and matricization, to matrix $\mathbf{G}_{(3)}$ whereas local structure of the image is lost; (*ii*) matrix factorization $\mathbf{G}_{(3)} = \mathbf{A}\mathbf{F}_{(3)}$ employed by linear mixing models (2) and (3) suffers from indeterminacies because $\mathbf{A}\mathbf{T}\mathbf{T}^{-1}\mathbf{F}_{(3)} = \mathbf{G}_{(3)}$ for any invertible **T**. It implies that infinitely many (**A**, $\mathbf{F}_{(3)}$) pairs can give rise to $\mathbf{G}_{(3)}$. In my notation *J* rows of $\mathbf{F}_{(3)}$ represent vectorized version of the original image **F** and its spatial derivatives, i.e. $\mathbf{F}_{(3)} \in \mathbb{R}^{J \times I_1 I_2}$. *J* represents unknown number of latent variables (original image and its spatial derivatives) in the linear mixture models (2) and (3). Meaningful solution of the factorization of $\mathbf{G}_{(3)}$ is characterized with $\mathbf{T}=\mathbf{P}\mathbf{\Lambda}$ where **P** is permutation matrix and $\mathbf{\Lambda}$ is diagonal matrix. These standard blind decompositions indeterminacies are obtained by imposing sparseness constraints on $\mathbf{F}_{(3)}$ by NMF algorithms [5] and statistical independence constraints by ICA algorithms [7]. Sparseness constraints imply that original image **F** and its spatial derivatives $\mathbf{F}_{i_1}$, $\mathbf{F}_{i_2}$, etc. do not occupy the same pixel and that is in general case not true. Statistical independence assumption is also not true as already observed in [5,7,8]. To improve statistical independence between the original image and its spatial derivatives I have used in [7] wavelet packets based transform to find out narrow subband where latent variables are least dependent. Due to this further convolution (multiscale filtering), as

correctly observed in [8], much more terms in Taylor series expansion are required to get good reconstruction than when no filtering is used. When using 3D TF approach to BID no such complications arise, because no constraints on latent variables need to be imposed in order to achieve unique factorization. For the purpose of blind decomposition of multi-channel image tensor $\underline{\mathbf{G}}$ we adopt Tucker3 model [11]:

$$\underline{\mathbf{G}} \approx \underline{\mathbf{R}} \times_1 \mathbf{A}^{(1)} \times_2 \mathbf{A}^{(2)} \times_3 \mathbf{A}^{(3)} \tag{4}$$

where $\underline{\mathbf{R}} \in \mathbb{R}^{J_1 \times J_2 \times J_3}$ is core tensor, $\left\{\mathbf{A}^{(n)} \in \mathbb{R}^{I_n \times J_n}\right\}_{n=1}^{3}$ are factors and $\times_n$ denotes n-mode product of a tensor with a matrix $\mathbf{A}^{(n)}$. The result of $\underline{\mathbf{R}} \times_n \mathbf{A}^{(n)}$ is a tensor of the same order as $\underline{\mathbf{R}}$ but the size J_n replaced by I_n. PARAFAC model [12], also called CANDECOMP [13], is a special case of Tucker3 model when $\underline{\mathbf{R}}$ is superdiagonal tensor with all elements zero except those for which all indices are the same. Compared to PARAFAC, Tucker3 model is more flexible due to the core tensor which allows interaction of a factor with any factor in the other modes [14]. In PARAFAC model factors in different modes can only interact factorwise. However, this restriction enables uniqueness of tensor factorization based the PARAFAC model within the permutation and scaling indeterminacies of the factors under very mild conditions [15,16]. There is no need to impose constraints on them such as sparseness or statistical independence. Assuming that $J_1=J_2=J_3=J$ and $J \le I_3$ uniqueness condition is reduced to $k_{\mathbf{A}^{(1)}} + k_{\mathbf{A}^{(2)}} + k_{\mathbf{A}^{(3)}} \ge 2J + 3$, where $k_{\mathbf{A}^{(n)}}$ is Kruskal rank of factor $\mathbf{A}^{(n)}$ [15,16]. Due to interaction between the factors there is no such theoretical guarantee on the uniqueness of tensor factorization based on Tucker3 model. However, despite of this Tucker3 model has been used successfully in hyperspectral image

analysis for dimensionality reduction, de-noising and target detection [17,18]. To identify original image and its spatial derivatives we refer to linear mixture model used in (2) and (3):

$$\mathbf{G}_{(3)} \approx \mathbf{A}\mathbf{F}_{(3)} \tag{5}$$

where columns of $\mathbf{A} \in \mathbb{R}^{I_3 \times J}$ represent weighting coefficients of the J images resident in the multi-channel image $\mathbf{G}_{(3)}$ while rows of $\mathbf{F}_{(3)} \in \mathbb{R}^{J \times I_1 I_2}$ represent vectorized versions of the original image and its spatial derivatives. Without constraints there are infinitely many decompositions satisfying model (5). From Tucker3 model (4) and linear mixture model (5) matrix of weighting coefficients and tensor of source image and its spatial derivatives $\underline{\mathbf{F}}$ are identified as

$$\begin{aligned} &\mathbf{A} \approx \mathbf{A}^{(3)} \\ &\underline{\mathbf{F}} \approx \underline{\mathbf{R}} \times_1 \mathbf{A}^{(1)} \times_2 \mathbf{A}^{(2)} \approx \underline{\mathbf{G}} \times_3 \left(\mathbf{A}^{(3)}\right)^{\dagger} \end{aligned} \tag{6}$$

where $\underline{\mathbf{F}} \in \mathbb{R}^{I_1 \times I_2 \times J}$ and '†' denotes Moore-Penrose pseudo-inverse. What remains after *3*-mode multiplication of the image tensor $\underline{\mathbf{G}}$ with pseudoinverse of array factor $\mathbf{A}^{(3)}$ is first part of (6). According to (5) this must be $\underline{\mathbf{F}}$. Second part of (6) is much less sensitive on numerical errors due to the fact that only one reconstructed quantity, array factor $\mathbf{A}^{(3)}$, takes places into reconstruction of $\underline{\mathbf{F}}$. This completes derivation of 3D TF-based SF BID algorithm that is defined without using any *a priori* information about the blurring process or source image. To estimate array factor $\mathbf{A}^{(3)}$ from image tensor $\underline{\mathbf{G}}$ based on Tucker3 model (4) I have used `tucker_als` function made available as a part of MATLAB Tensor Toolbox [20]. $\underline{\mathbf{F}}$ is then reconstructed through *3*-mode multiplication of the image tensor $\underline{\mathbf{G}}$ and pseudoinverse of $\mathbf{A}^{(3)}$. `tucker_als` function relies on mean squared error minimization implemented in alternating least square fashion [19]. I demonstrate performance of 3D TF-based SF BID on experimental RGB image shown in Figure 1 with dimensions of 384×512 pixels i.e. I_1=384 and I_2=512. It has been

recorded by digital camera in manually defocused mode. This image yields spatially invariant degradation that complies with fundamental property of convolution equation (1). Thus, it can be used for the proof-of-principle of proposed SF BIF algorithm. The same image has been used previously in [5,7] in gray scale version. Here, I use color version to demonstrate versatility of the 3D TF SF BID method. Color image is deconvolved by applying described algorithm to each spectral image separately. Figure 2 shows deconvolution result obtained by 3D TF SF BID algorithm. This result was obtained by setting the number of latent variables in (4) to J=5. However, varying J between 3 and 16 yielded result of the, in principle, same quality. Figure 3 shows results obtained by wavelet packets based subband decomposition ICA (WP SDICA) algorithm [7] where restoration errors are in part due to image vectorization process and mainly due to multiscale filtering necessary to satisfy statistical independence constraint imposed on the latent variables in the linear mixture model (5). Due to space limitation I did not carry out comparative performance analysis between TF SF BID method and blind Richardson-Lucy and NMF-based methods. However, based on results reported in [7] it might be concluded that TF-based method would compare favorably against them.

This work was partially supported through grant 098-0982903-2558 funded by the Ministry of Science, Education and Sports, Republic of Croatia.

References:

1. M.R. Banham, and A.K. Katsaggelos, "Digital Image Restoration," IEEE Signal Process. Mag. **14**, 24 (March, 1997).

2. D. Kundur, and D. Hatzinakos, "Blind Image Deconvolution," IEEE Signal Process. Mag. **13**, 43 (May, 1996).

3. P. Campisi, K. Egiazarian, editors, *Blind Image Deconvolution* (CRC Press, Boca Raton, 2007).

4. M.M. Bronstein, A. Bronstein, M. Zibulevsky, and Y.Y. Zeevi, "Blind Deconvolution of Images Using Optimal Sparse Representations," IEEE Tr. on Image Processing **14**, 726 (2005).

5. I. Kopriva, "Single Frame Multichannel Blind Deconvolution by Non-negative Matrix Factorization with Sparseness Constraint," Opt. Letters **30**, 3135 (2005).

6. A. Hyvärinen, J. Karhunen, and E. Oja, *Independent Component Analysis* (Wiley Interscience, 2001).

7. I. Kopriva, "Approach to Blind Image Deconvolution by Multiscale Subband Decomposition and Independent Component Analysis," J. Opt. Soc. Am. A **24**, 973 (2007).

8. C. Yi-nan, J. Wei-qi, W. Ling-Xue, Z. Lei, Y. Hong-sheng, "A Gabor subband decomposition ICA and MRF hybrid algorithm for infrared image reconstruction from subpixel shifted sequences," Opt. Commun. **282**, 786 (2009).

9. S. Umeyama, Scripta Technica, "Blind Deconvolution of Blurred Images by Use of ICA" Electron Comm Jpn, Pt 3, **84**(12), 1 (2001).

10. H. A. L. Kiers, "Towards a standardized notation and terminology in multiway analysis," J. Chemometrics **14**, 105 (2000).

11. L. R. Tucker, "Some mathematical notes on three-mode factor analysis," Psychometrika **31**, 279 (1966).

12. J. D. Carrol, and J. J. Chang, "Analysis of individual differences in multidimensional scaling via N-way generalization of Eckart-Young decomposition," Psychometrika **35**, 283 (1970).

13. R. A. Harshman, "Foundations of the PARAFAC procedure: models and conditions for an exploratory multi-mode factor analysis," UCLA Working Papers in Phonetics **16**, 1 (1970).

14. E. Acar, and B. Yener, "Unsupervised Multiway Data Analysis: A Literature Survey," IEEE Trans. Knowl. Data Eng. **21**, 6 (2009).

15. J. B. Kruskal, "Three-way arrays: Rank and uniqueness of trilinear decompositions," Linear Algebra Appl. **18**, 95 (1977).

16. N. D. Sidiropoulos, and R. Bro, "On the uniqueness of multilinear decomposition of *N*-way arrays," J. of Chemometrics **14**, 229 (2000).

17. N. Renard, S. Bourennane, and J. Blanc-Talon, "Denoising and Dimensionality Reduction Using Multilinear Tools for Hyperspectral Images," IEEE Geosci. Remote Sens. Lett. **5**, 138 (2008).

18. N. Renard, and S. Bourennane, "Improvement of Target Detection Methods by Multiway Filtering," IEEE Trans. Geosci. Remote Sens. **46**, 2407 (2008).

19. L. De Lathauwer, B. De Moor, and J. Vandewalle, "A multilinear singular value decomposition," SIAM J. Matrix Anal. and Appl. **21**, 1253 (2000).

20. B. W. Bader, and T. G. Kolda, *MATLAB Tensor Toolbox version 2.2.* http://csmr.ca.sandia.gov/~tkolda/TensorToolbox.

Figure Captions:

Figure 1. RGB experimental image obtained by digital camera in manually defocused mode.

Figure 2. RGB image restored by 3D TF SF BID algorithm.

Figure 3. RGB image restored by WP SDICA BID algorithm [7].

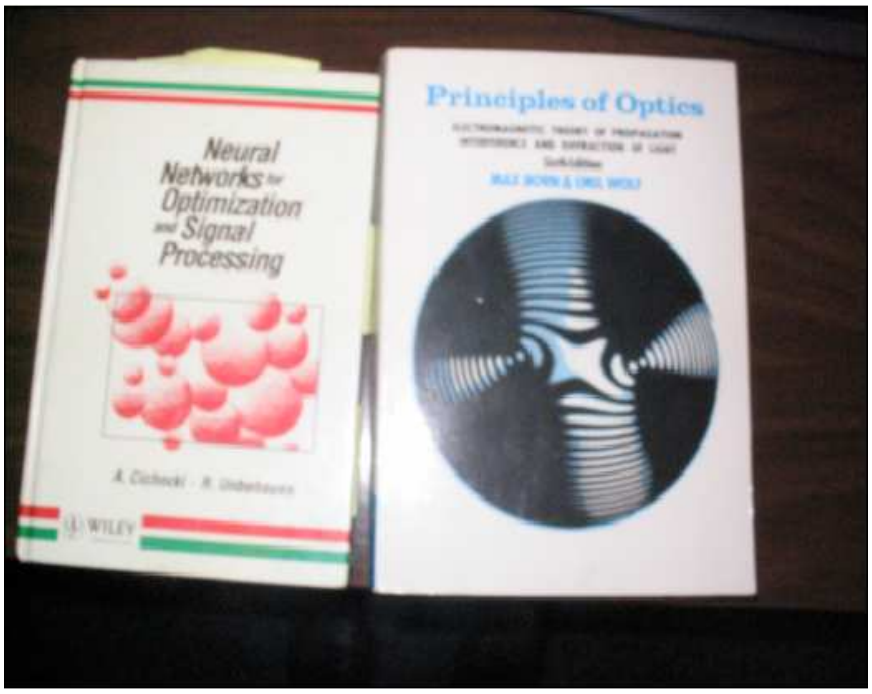

Fig. 1, OL, Kopriva

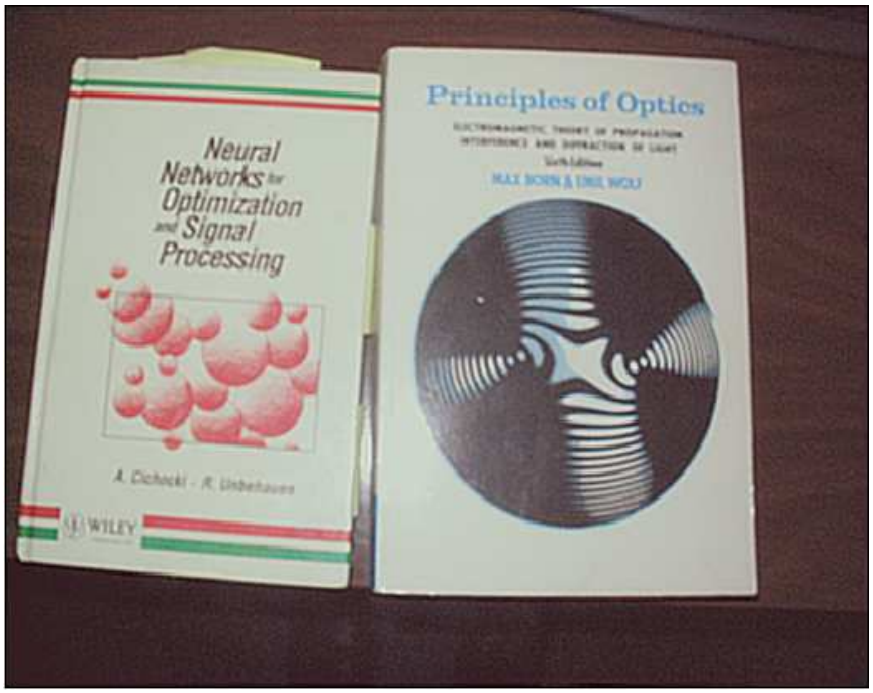

Fig. 2, OL, Kopriva

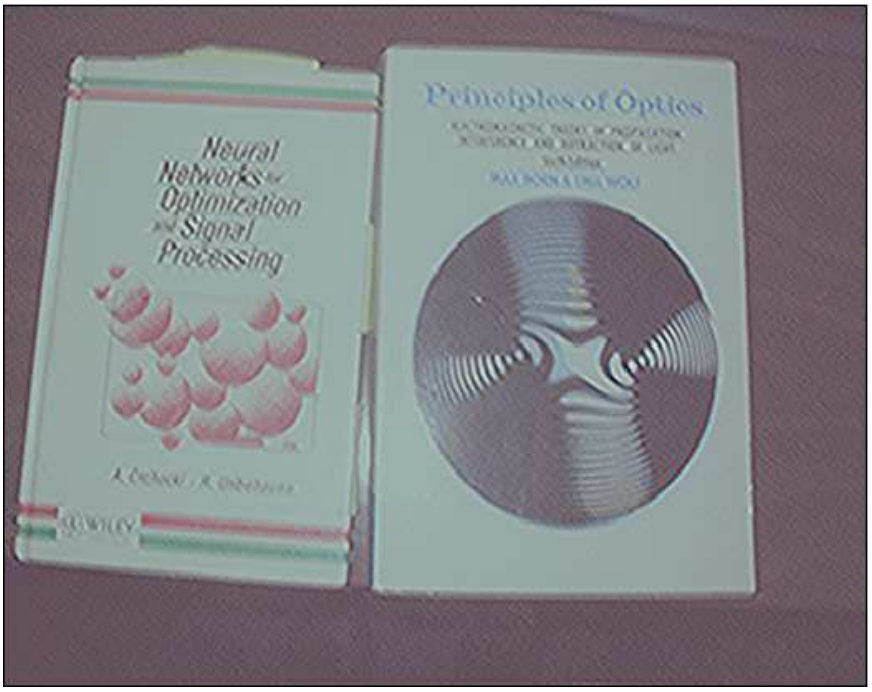

Fig. 3, OL, Kopriva